

The Spectrum of the 2+1 Dimensional Gauge Ising Model

V. Agostini^a, G. Carlino^a, M. Caselle^{a*} and M. Hasenbusch^{b†}

^a *Dipartimento di Fisica Teorica dell'Università di Torino
Istituto Nazionale di Fisica Nucleare, Sezione di Torino
via P.Giuria 1, I-10125 Torino, Italy*

^b *Humboldt Universität zu Berlin, Institut für Physik
Invalidenstr. 110, D-10099 Berlin, Germany*

Abstract

We present a high precision Monte Carlo study of the spectrum of the Z_2 gauge theory in $2 + 1$ dimensions in the strong coupling phase. Using state of the art Monte Carlo techniques we are able to accurately determine up to three masses in a single channel. We compare our results with the strong coupling expansion for the lightest mass and with results for the universal ratio σ/m^2 determined for the ϕ^4 -theory. Finally the whole spectrum is compared with that obtained from the Isgur-Paton flux tube model and the spectrum of the $2 + 1$ dimensional $SU(2)$ gauge theory. A remarkable agreement between the Ising and $SU(2)$ spectra (except for the lowest mass state) is found.

*e-mail: caselle@to.infn.it

†e-mail: hasenbus@birke.physik.hu-berlin.de

1 Introduction

This paper is devoted to the study of the glueball spectrum in the three dimensional gauge Ising model. There are two main reasons for which this model is interesting. The first one is that, as it is well known, the infrared regime of Lattice Gauge Theories (LGT) in the confining phase displays a large degree of universality. Hence it is quite convenient to study such universal infrared behaviour in the case of the three dimensional Ising gauge model, which is the simplest (but nevertheless non-trivial) possible lattice gauge theory and allows high precision Montecarlo simulations with a relatively small amount of CPU time. The main evidence in favour of the above mentioned universality is given by the Wilson loop behaviour, whose functional form does not depend on the choice of the gauge group, and shows a rather simple dependence on the number of space-time dimensions. Both these features are commonly understood as consequences of the fact that the relevant degrees of freedom in the confining regime are string-like excitations. Such a string description is still not well understood, the theory being anomalous at the quantum level. For instance, it is absolutely not clear how to translate at the string level the choice of the gauge group and which is the correct string Lagrangian. However it is widely believed that in the infrared regime, as the interquark distance increases all these different string theories flow toward a common fixed point which is not anomalous and corresponds to the two dimensional conformal field theory of $(d-2)$ free bosons ($d-2$ being the number of transverse dimensions of the original string theory) [1]. The phenomenological models which try to keep into account this string-like picture are usually known as “flux-tube” models. They have proved to be very efficient in describing the behaviour of the Wilson loop and in particular of its quantum fluctuations [2, 3]. Moreover, the interquark potential that one obtains with these models gives a good description of the spectrum of heavy quarkonia [4, 5]. As an example of the strategy discussed above in [6, 7] some flux tube predictions on the behaviour of Wilson loops were successfully tested with high precision simulations in the three dimensional gauge Ising models. These studies allowed to obtain a clear insight in the fine structure of the flux tube model.

In the case of the glueball spectrum the situation is less clear. A string-inspired model exists also for the glueball spectrum: the Isgur Paton model (IP in the following). However in this case the equivalent of the interquark distance for the Wilson loop is missing. In other words, it is not obvious to find a length scale above which one can think to have reached a common universal infrared behaviour.

For this reason it would be very interesting to test if the same universality (which, as mentioned above, should manifest itself as a substantial independence from the choice of the gauge group) displayed by the Wilson loops also holds for the glueball spectrum. This can be more easily studied in the (2+1) dimensional case, for which some relevant simplifications occur in the spectrum (see below) and a much higher precision can be achieved in the Montecarlo simulations. Recently the glueball spectrum was obtained for the (2+1) dimensional SU(2) gauge model [8, 9].

In this paper we shall present the spectrum in the case of the (2+1) Ising gauge model. The comparison between the SU(2) and Ising spectra shows that, not only the pattern of the states is the same in the two models, but also the values of the masses (except for the lowest state) are in remarkable agreement. This is a strong evidence in favour of the above mentioned universality, and suggests that the higher states of the glueball spectrum of any LGT, (as it happens for the behaviour of large enough Wilson loops) can be predicted by some relatively simple flux-tube inspired model. The simplest possible model of this type is the IP model. So we shall devote the last part of this paper to a detailed comparison with its predictions.

A second important reason of interest in the gauge Ising model is that it is related by duality to the ordinary three dimensional spin Ising model. As a consequence, the glueball spectrum is mapped in the spectrum of massive excitations of the spin Ising model. The knowledge of the spectrum can teach us a lot on the physics of the model (this is the lesson that we have learnt from the S-matrix approach to two dimensional field theories) and also allows a non trivial check of our results with the predictions of the ϕ^4 description of the spin Ising model. In particular we shall use the value of the lowest mass excitation: $1/\xi$ (which coincides with the 0^+ glueball state of the dual gauge model), which we can measure with very high precision, to test our simulations. We shall compare our results for the correlation length ξ with those obtained with the longest available strong coupling series and with some recent calculations with the ϕ^4 model. Indeed, the behaviour of the correlation length in the broken phase of the 3d Ising model and its comparison with the correlation length in the high temperature phase and with its second momentum approximation is a very interesting problem in itself. We shall discuss this topic in detail in a separate paper [10].

This paper is organized as follows: Sect. 2 and 3 are devoted to a description of the model that we have studied and of the details of our simulations. In sect. 4 we report our results on the lowest mass excitation and compare them with some existing predictions. Sect. 5 is devoted to a description of our estimates for the full spectrum and to a comparison with existing data on SU(2) and with the Isgur Paton model. The last section is devoted to some concluding remark.

2 General Setting

2.1 The Models

We take a lattice of N_t (N_s) spacings in the time (space) direction. Periodic boundary conditions are imposed in time and in space directions. The gauge fields are described by the link variables $g_{n;\mu} \in -1, 1$, where $n \equiv (\vec{x}, t)$ denotes the space-time position of the link and μ its direction. We choose for simplicity the same bare

coupling β in the time and space directions. The Wilson action is then

$$S_{gauge} = -\beta \sum_{n,\mu < \nu} g_{n;\mu\nu} \quad (1)$$

where $g_{n;\mu\nu}$ are the plaquette variables, defined as usual by

$$g_{n;\mu\nu} = g_{n;\mu} g_{n+\mu;\nu} g_{n+\nu;\mu} g_{n;\nu} \quad . \quad (2)$$

The Ising spin model in 2+1 dimensions is defined by the action

$$S_{spin} = -\tilde{\beta} \sum_{n,\mu} s_n s_{n+\mu} \quad , \quad (3)$$

where the field variable s_n takes the values -1 and $+1$.

The Kramers–Wannier duality transformation relates the two partition functions:

$$\begin{aligned} Z_{gauge}(\beta) &\propto Z_{spin}(\tilde{\beta}) \\ \tilde{\beta} &= -\frac{1}{2} \log [\tanh(\beta)] \quad . \end{aligned} \quad (4)$$

Using the duality transformation it is possible to build up a one-to-one mapping of physical observables of the gauge system onto the corresponding spin quantities.

In the following we shall use this duality transformation to relate the lowest state of the spectrum of the gauge Ising model: the 0^+ glueball, to the correlation length of the spin Ising model, for which several predictions, both from strong coupling expansions and from the ϕ^4 theory exist.

Another important consequence of duality is that the string tension of the gauge Ising model is mapped into the interface tension of the Ising spin model. In the following we shall denote both them with the same symbol σ .

2.2 The algorithm

For the determination of the spectrum in the broken phase of the gauge model we used a (gauge version) of the microcanonical demon algorithm [11].

In our simulation the microcanonical demon algorithm of [11] was combined with a particularly efficient canonical update of the demons [12] in order to obtain the canonical ensemble of the gauge model. This algorithm was implemented in the multispin coding technique. The demons are auxiliary degrees of freedom that are added to the system. One considers the combined action

$$S = \sum_{\alpha=1}^{bit} S_{gauge}^{\alpha} + S_D^{\alpha} \quad , \quad (5)$$

where $bit = 64$ independent copies of the gauge model and the demon system are simulated. The demon action is given by

$$S_D = \beta \sum_{n,\mu} d_{n;\mu} \quad , \quad (6)$$

where the demon takes the values $0, 2, \dots, d_{max}$. For our simulations we have chosen $d_{max} = 6$. The updates performed are similar to standard Metropolis updates. First a change of the sign of a given link variable $g_{n,\mu}$ is proposed. Then the corresponding change of the action of the gauge model $\Delta S_{gauge} = S'_{gauge} - S_{gauge}$ is computed. If $d_{n,\mu} - \Delta S_{gauge}$ is in the allowed range of the demon then the proposal for the link variable is accepted and the value of the demon is changed to $d'_{n,\mu} = d_{n,\mu} - \Delta S_{gauge}$. Performing such updates once for all μ and n is called one "sweep" in the following.

In order to simulate the canonical ensemble of the model the microcanonical updates are interleaved with canonical updates of the demon system. The demon with $d_{max} = 6$ can be thought of as a sum of two two-state demons with the energies 0; 2 and 0; 4 respectively.

The demon-update is done separately for these two demon-species. First a new total number E of exited demons is chosen with a probability proportional to the Boltzmann-weight

$$P(E) \propto \frac{N_D!}{(N_D - E)! E!} \exp(-\bar{\beta}E) \quad , \quad (7)$$

where $N_D = 64 \times 3 \times N_t \times N_s^2$ is the total number of demons, E the number of demons in the exited state and $\bar{\beta} = 2\beta$ or $\bar{\beta} = 4\beta$ for the two demon species respectively.

Next if $N_c = E_{new} - E_{old} > 0$ then N_c randomly chosen demons with $d = 0$ are updated to $d = 2, 4$ respectively else $-N_c$ randomly chosen demons with $d = 2, 4$ are updated to $d = 0$.

In addition we performed translations of the demons on the lattice and shifts along the 64 gauge systems.

The method discussed above is, up to our knowledge, the first attempt to construct a microcanonical demon algorithm for a gauge model and has proved to be a very powerful tool. For moderate correlation lengths, as discussed in this paper, it should provide superior performances compared to a cluster-update [13]. A careful quantitative study of this question is in progress [14].

3 The simulation

3.1 Determination of the Spectrum.

In general the mass-spectrum of a theory is given by the eigenvalues of the Hamiltonian of the theory. The discrete version of the Hamiltonian on the lattice is called transfer matrix T . For a finite lattice the transfer matrix of the Ising model is a real symmetric matrix. Therefore it can be diagonalized. Let us denote the resulting eigenvalues by λ_i . Then the mass-spectrum is given by

$$m_i = -\log \left(\frac{\lambda_i}{\lambda_0} \right) \quad , \quad (8)$$

where λ_0 is the largest eigenvalue of T . For sufficiently small system sizes the eigenvalues of T can be computed by numerically diagonalizing T . In the case of the 2+1 dimensional Ising spin model one can reach at most lattices of size $5^2 \times \infty$ [15] this way. For larger lattice sizes one has to rely on Monte Carlo techniques. The basic strategy is to compute expectation values of certain correlation functions. Masses can then be determined from the decay of these correlation functions with the separation in time.

$$\begin{aligned}
G(t) &= \langle A(0)B(t) \rangle = \frac{\langle 0|AT^tB|0 \rangle}{\langle 0|T^t|0 \rangle} \\
&\sim \frac{1}{\lambda_0^t} \sum_i \langle 0|A|i \rangle \langle i|T^t|j \rangle \langle j|B|0 \rangle = \sum_i c_i \left(\frac{\lambda_i}{\lambda_0} \right)^t = \sum_i c_i \exp(-m_i t) \quad (9)
\end{aligned}$$

where $|i\rangle$ denotes the eigenstates of the transfer matrix and

$$c_i = \langle 0|A|i \rangle \langle i|B|0 \rangle . \quad (10)$$

The main problem in the numerical determination of masses is to find operators A and B that have a good overlap with a single state $|i\rangle$; i.e. that c_i is large compared with c_j , $j \neq i$. The first, important, step in this direction is to realize that, by choosing the symmetry properties of the operators A and B properly, we can select channels; i.e. we can choose, for example, A and B such that all the c_i 's vanish except those corresponding to, say, a given value of the angular momentum. Due to its importance, we devote the next section to a detailed discussion of the choice and construction of the lattice operators. By using so called ‘‘zero momentum’’ operators, namely operators obtained by summing over a slice orthogonal to the time direction, all c_i 's that correspond to nonvanishing momentum vanish.

A systematic way to further improve the overlap is to study simultaneously the correlators among several operators A_α that belong to the same channel. This is indeed a natural prescription in the context of the glueball physics since the glueballs are expected to be extended objects and choosing several extended operators on the lattice one can hope to find a better overlap with the (unknown) glueball wave function. One must then measure all the possible correlations among these operators and construct the crosscorrelation matrix defined as:

$$C_{\alpha\beta}(t) = \langle A_\alpha(t)A_\beta(0) \rangle - \langle A_\alpha(t) \rangle \langle A_\beta(0) \rangle \quad (11)$$

By diagonalizing the crosscorrelation matrix one can then obtain the mass spectrum.

This method can be further improved[16, 17] by studying the generalized eigenvalue problem

$$C(t)\psi = \lambda(t, t_0)C(t_0)\psi \quad (12)$$

where t_0 is small and fixed (say, $t_0 = 0$). Then it can be shown that the various masses m_i are related to the generalized eigenvalues as follows [16, 17]:

$$m_i = \log \left(\frac{\lambda_i(t, t_0)}{\lambda_i(t+1, t_0)} \right) \quad (13)$$

where both t and t_0 should be chosen as large as possible, $t \gg t_0$ and as t is varied the value of m_i must be stable within the errors. Practically one is forced to keep $t_0 = 0, 1$ to avoid too large statistical fluctuations and at the same time t is in general forced to stay in the range $t = 1$ to 7 , depending on β and the channel, to avoid a too small signal to noise ratio. This method is clearly discussed in [16, 17] and we refer to them for further details. All the results that we shall list below for the glueball spectrum have been obtained with this improved method. In order to give some informations on the reliability of the estimates we shall also list, besides the numerical values of the masses, the pair (t_0, t) used to extract them.

3.2 Choice of operators.

The various glueball masses are labelled by their angular momentum. Thus, in order to distinguish the various states of the spectrum one must construct operators with well defined angular momentum. The fact that we are working in (2+1) dimensions makes this construction rather non trivial, and definitely different from the (3+1) dimensional case. Moreover, since we are working on a cubic lattice, where only rotations of multiples of $\pi/2$ are allowed, we must study the symmetry properties of our operators with respect to a finite subgroup of the two-dimensional rotations. Let us first ignore the effect of the lattice discreteness and deal with the peculiar features which, already in the continuum formulation, the (2+1) Ising (and SU(2), which is completely equivalent in this respect) spectrum has with respect to the (3+1) dimensional SU(3) spectrum. These features have been discussed for the SU(2) model in ref. [8, 9] to which we refer for further details. We shall summarize here only the main results.

- a] For the Ising model, as for the SU(2) model, we cannot define a charge conjugation operator. The glueball states are thus labelled only by their angular momentum J and by their parity eigenvalue $P = \pm$. The standard notation is J^P
- b] In (2+1) dimensions it can be shown that all the states with angular momentum different from zero are degenerate in parity. Namely J^+ and J^- (with $J \neq 0$) must have the same mass.

On the cubic lattice the group of two dimensional rotations and reflections becomes the dihedral group D_4 . This group is non abelian, has eight elements and five irreducible representations. Four of these are one-dimensional irreps, the last one has dimension two. The group structure is completely described by the table of characters [18] which we have reported in tab.1 .

Table 1: *Character table for the group D_4*

	1	C_4^2	$C_4(2)$	$C_2(2)$	$C_{2'}(2)$
A_1	1	1	1	1	1
A_2	1	1	1	-1	-1
B_1	1	1	-1	1	-1
B_2	1	1	-1	-1	1
E	2	-2	0	0	0

In the top row of tab.1 are listed the invariant classes of the group, and in the first column the irreducible representations. We have followed the notations of [18] to label classes and representation (with the exception of the class containing the identity which we have denoted with **1** instead of the usual E to avoid confusion with the two-dimensional representation). The entries of the table allow to explicitly construct the various representations and hence also the lattice operators which we are looking for. The relationship of these operators with the various glueball states immediately follows from the group structure. In particular one can show that:

- a] Only operators with angular momentum $J \pmod{4}$ can be constructed. This is a common feature of all cubic lattice regularizations. It means that glueball states which in the continuum have values of J higher than 3 appear on the lattice as secondary states in the family of the corresponding $J \pmod{4}$ lattice operator.
- b] The four one-dimensional irreps are in correspondence with the J even states. More precisely:

$$0^+ \rightarrow A_1, \quad 0^- \rightarrow A_1, \quad 2^+ \rightarrow B_1, \quad 2^- \rightarrow B_2$$

This means that the discreteness of the lattice splits the degeneracy between 2^+ and 2^- which we discussed above. The splitting between these two states gives us a rough estimates of relevance of the breaking of the full rotational group due to the lattice discretization. As we shall see below this splitting is essentially zero within the errors, in agreement with our expectation that approaching the continuum limit the full continuum symmetries should be recovered. Notice however that this is a very non-trivial result since the operators associated to 2^+ and 2^- on the lattice turn out to be very different.

- c] All the odd parity states are grouped together in the two-dimensional irreducible representation E . This means that we cannot distinguish among them on the basis of the lattice symmetries. We can conventionally assume, say, that the $J = 3$ states have a mass lower than the $J = 1$ ones (this would agree with

the pattern which emerges from the Isgur-Paton model, see below), and that the $J = 1$ thus appear as secondaries in the $J = 3$ family. However in the following we shall avoid this assumption and shall denote the states belonging to this family as $J = 1/3$ states. In agreement with the above discussion, if the full rotational symmetry is recovered, we expect that the states belonging to this family are degenerate in parity and thus that the lowest mass states, which are the ones that we can measure more precisely appear as a doublet. This prediction will be in fact confirmed by our results.

The simplest lattice operators, constructed according to the character table, are shown in fig.1. Notice however that these are only a small subset of the operators that we actually measured in our simulations. In particular we studied 27 different operators for the 0^+ channel, and 15, 9, 5, 16 for the $2^+, 2^-, 0^-$ and $1/3$ channels respectively.

3.3 The data sample.

First we carefully checked for $\beta = 0.72484$ the dependence of the masses on the lattice size. In table 2 we give results for the 0^+ channel for various spatial extensions N_s of the lattice. The results become stable within our numerical accuracy for $N_s \geq 16$.

Table 2: *Study of finite size effects for the Z_2 gauge model at $\beta = 0.72484$ (which corresponds to $\beta = 0.2391$ for the spin model). 10000 measurements, $t = 3$. $N_t = 48$ throughout.*

N_s	ξ_{0+}	ξ'_{0+}	ξ''_{0+}
8	1.485(3)	0.699(7)	0.59(5)
10	1.408(3)	0.836(6)	0.52(2)
12	1.313(3)	0.800(7)	0.58(2)
16	1.298(3)	0.721(8)	0.53(3)
20	1.295(3)	0.717(8)	0.52(3)
24	1.296(3)	0.705(8)	0.52(3)

In order to be safe of finite size effects we have chosen $N_s \approx 15\xi_{0+}$ for the following simulations. We denote with N_t the “time” direction in which we calculate the correlations. In these simulations we have always chosen $N_t > N_s$.

Next we performed simulations for $\beta = 0.74057, 0.74883, 0.752023$ and 0.75632 (the corresponding (dual) couplings for the spin model are reported in tab. 3) on lattices of the size 72×36^2 , 60×40^2 , 70×50^2 and 100×70^2 . We performed 4790, 11890, 5000 and 2080 measurements on each of the 64 systems for the four β values respectively. A measurement was performed after 200, 200, 400 and 500

update-sweeps. We made no attempt to study carefully the autocorrelation times of Wilson-loops. Some rough tests indicate that they are of the same order as the number of update-sweeps which we performed for one measurement. All the information on our simulations are summarized in tab. 3.

The total amount of CPU-time for the run of the 100×70^2 lattice took about 55 days on a DEC 3000 Model 400 AXP Workstation. The ratio of CPU time spent in updating and measurement was about 3/1.

Table 3: *Some informations on the data sample for the glueball spectrum: β is the coupling constant of the gauge Ising model and $\tilde{\beta}$ the corresponding (dual) coupling for the spin model. N_t and N_s are the lattice sizes. With u.s. we denote the number of update sweeps between two measures and with m.s. the total number of measured sweeps.*

β	$\tilde{\beta}$	$N_t \times N_s^2$	u.s.	m.s.
0.74057	0.23142	72×36^2	200	4790
0.74883	0.22750	60×40^2	200	11890
0.75202	0.22600	70×50^2	400	5000
0.75632	0.22400	100×70^2	500	2080

Our results are collected in table 4. The data presented correspond to the inverse masses: $\xi_i \equiv \frac{1}{m_i}$. In the first row we have reported the dominant state for each family while in the subsequent rows are reported the various secondary excitations. For each mass we have also reported the pair (t_0, t) used to extract the mass from the data. When the statistical fluctuations were too large to obtain a meaningful statistical error, we tried to fix anyway an approximate estimate for the masses. In the tables these estimates are reported in square brackets, to remind that they are certainly affected by large errors. Empty boxes denote the cases in which even this approximate estimate was impossible to find. Looking at the data one can immediately see the announced degeneration of the 2^+ and 2^- families and the fact that the first two states of the $1/3$ family appear as a doublet.

4 The lowest mass state

4.1 Comparison with strong coupling expansions

In this section we concentrate on the lowest mass state: the 0^+ glueball. As mentioned above this state coincides with the inverse of the correlation length ξ of the spin Ising model. For this observable, very long strong coupling series have recently been obtained by H.Arisue and K.Tabata [19]. To extract from these series estimates for ξ at the values of β in which we are interested in we used the so called

Table 4: *Glueball spectrum. The discussion is given in the text.*

β	0^+	0^-	2^+	2^-	$1/3$
0.74057	(0,3) 1.864(5)	(0,2) 0.60(5)	(0,2) 0.77(1)	(0,2) 0.75(1)	(0,1) [0.46]
	(0,3) 1.03(2)	(0,1) [0.42]	(0,2) 0.65(2)	(0,2) [0.60]	(0,1) [0.46]
	(0,2) 0.77(2)	(0,1) [0.37]	(0,2) [0.60]	(0,1) [0.44]	(0,1) [0.38]
0.74883	(0,3)(1,2) 2.592(5)	(0,2)(1,2) [0.75]	(0,2)(1,2) 1.04(2)	(0,3)(1,2) 1.05(3)	(0,2)(1,1) 0.66(3)
	(0,2)(0,3) 1.42(1)		(0,2) [0.82]	(0,2)(1,2) 0.82(3)	(0,2)(1,1) 0.63(3)
	(0,3) 1.06(2)			(0,2)(1,2) [0.63]	(0,1)(1,1) [0.50]
0.75202	(0,4)(1,3) 3.135(9)	(0,3) 0.96(7)	(0,3)(1,3) 1.27(4)	(0,3)(1,3) 1.23(3)	(0,3) 0.8(1)
	(0,4)(1,2) 1.72(1)	(0,2) 0.69(3)	(0,3)(1,3) 1.00(5)	(0,4)(1,3) 1.0(1)	(0,3) 0.8(1)
	(0,4) 1.20(4)	(0,2) [0.65]	(0,1)(0,2) [0.8]	(0,2) [0.72]	(0,2) [0.62]
0.75632	(0,7)(1,4) 4.64(3)	(0,2) [1.1]	(0,4)(1,2) 1.76(3)	(0,4) 1.69(3)	(0,3)(1,2) 1.2(1)
	(0,5)(1,3) 2.50(3)	(0,1) [0.80]	(0,3)(1,2) 1.39(3)	(0,3)(1,2) 1.38(5)	(0,3)(1,2) 1.1(1)
	(0,4)(1,2) 1.72(4)	(0,1) [0.58]	(0,3) [1.07]	(0,2)(1,2) 1.1(1)	(0,2)(1,1) [0.9]

“double biased inhomogeneous differential approximants” (IDA). The techniques of IDA is well described in [20, 21], to which we refer for notations and further details. In order to keep the fluctuations of the results under control, we have chosen to use double biased IDA, namely we have fixed both the critical coupling and ν to their most probable values $\beta_c = 0.221655$ and $\nu = 0.63$ [22] (for a discussion of these double biased IDA see again ref. [21]). Following ref. [21] we use the notation [K/L;M] for the approximants. In fig.2 approximants of ξ at $\beta = 0.75632$ are given for a large range of [K/L;M]. Certainly the values for ξ are centered around a value of about 4.6, which is consistent with our Montecarlo result. We made no attempt to extract an error-estimate from the spread of the values of the IDA’s.

In table 5 results for $\beta = 0.72484, 0.74057, 0.74883, 0.75202$ and 0.75632 for three choices of K,L,M which give estimates consistent with our Montecarlo estimate for

$\beta = 0.75632$ are summarized.

For comparison we give in addition the values of ξ in the last column, which are taken from tab. 2 and table 4. The important observation is, that these three

Table 5: *Comparison with the strong coupling expansion*

β	$\tilde{\beta}$	[4/6;7]	[6/6;5]	[6/5;6]	ξ
0.72484	0.23910	1.2995	1.2998	1.2977	1.296(3)
0.74057	0.23142	1.8739	1.8751	1.8699	1.864(5)
0.74883	0.22750	2.5946	2.5974	2.5876	2.592(5)
0.75202	0.22600	3.1299	3.1343	3.1208	3.135(9)
0.75632	0.22400	4.6237	4.6325	4.6084	4.64(3)

approximants also give results that are consistent with our Montecarlo estimates for $\beta = 0.72484, 0.74057, 0.74883$ and 0.75202 .

4.2 Scaling behaviour and ϕ^4 theory

In the neighbourhood of the critical temperature the correlation length in the low temperature phase of the spin Ising model scales as

$$\xi \sim f_- \left(\frac{\tilde{\beta} - \tilde{\beta}_c}{\tilde{\beta}_c} \right)^{-\nu} . \quad (14)$$

Most of the recent estimates for the critical exponent ν range from 0.629 to 0.632 [22], however in a recent MCRG study $\nu = 0.625(1)$ was found [23]. This uncertainty can be eliminated by looking at adimensional combinations like $\sigma\xi^2$ (where σ denotes the interfacial tension in the spin model or, equivalently, the string tension in the gauge model). In the scaling limit this product should be constant. An interesting feature of this adimensional product is that its value in the continuum limit can be evaluated in the framework of the ϕ^4 theory [24], which gives:

$$\sigma\xi^2 = 0.1024(88) \quad (15)$$

Recently, very precise estimates of σ have been obtained in the same range of β values in which we are interested [26, 27]¹. The results obtained by using these values and our estimates of ξ are reported in tab.6.

The value of $\sigma\xi^2$ increases as β approaches its critical value. This trend is the signature of the presence of a correction to scaling term. This type of corrections

¹The values of σ for $\tilde{\beta} = 0.2391, 0.2314$ and 0.2260 are obtained by interpolation of nearby values. The quoted errors take also into account the systematic uncertainty due to the fact that we only know the first non-Gaussian contributions in the functional form of the interface tension (see [27] for a discussion).

Table 6: *Scaling behaviour of ξ . In the second column we report the values of σ extracted from [26] and [27].*

$\tilde{\beta}$	σ	$\sigma\xi^2$
0.23910	0.05558(10)	0.0934(6)
0.23142	0.02752(10)	0.0956(9)
0.22750	0.01473(10)	0.0990(11)
0.22600	0.01011(10)	0.0994(16)
0.22400	0.00478(10)	0.1029(34)

is always present (see for instance the discussion in [21]) but becomes visible only if the data sample is precise enough. We expect the following behaviour for $\sigma\xi^2$:

$$\sigma\xi^2 = (\sigma\xi^2)_0 + \rho\xi^{-\omega} \quad (16)$$

where $\omega \approx 0.8$ [22]. $(\sigma\xi^2)_0$ is the continuum limit value and ρ an unknown constant. Fitting our five data with eq.(16) we find: $\rho = -0.015(3)$ and $(\sigma\xi^2)_0 = 0.1056(19)$ with a reduced χ^2 : $\chi_{red}^2 = 0.42$ which corresponds to a confidence level of 70%. This continuum limit value for $(\sigma\xi^2)_0$ is in perfect agreement with the ϕ^4 prediction of eq.(15). It also implies that $m_{0^+}/\sqrt{\sigma} = 3.08(3)$. We shall use this result in the following section. Recently S.-Y. Zinn and M.E. Fisher [25] published a rather smaller result: $\sigma\xi^2 = 0.0965(20)$, based on the data of ref. [26] and a low temperature expansion. However most of the discrepancy between their result and our one can be explained by the fact that they use, in contrast to us, the second moment correlation length.

5 The whole glueball spectrum

5.1 Numerical Results

In order to obtain a meaningful result for the continuum theory we have to measure the various masses of the spectrum in physical units. Commonly the (square root of the) string tension is used for this purpose. Our results are reported in tab. 7 where we used the σ -values listed in tab.6. It can be seen that the scaling behaviour is well established within the statistical errors for the whole spectrum (except for the lowest state that we have discussed in the previous section). Thus, to extract the continuum values (except for 0^+) we have chosen the simplest possible attitude, and took the weighted mean of the masses at the four values of β as our final result. If we assume that corrections to scaling are of about the same size as for the 0^+ state, where we have the by far most accurate results, this procedure is justified. These continuum values are reported in the sixth column of tab. 7. In the last column

we have reported, for the reader's convenience the continuum values of the masses measured in units of the lowest mass 0^+ . With the notation $(J^P)'$ and $(J^P)''$ we denote the second and third excitation in the J^P channel. The continuum value for the 0^+ state, reported in tab.7 is that extracted in the previous section.

Table 7: *The glueball spectrum in units of the square root of the string tension. In the sixth column we report our extrapolation to the continuum limit. In the last column we report the same quantity, measured in units of the lowest excitation.*

J^P	$\beta = 0.74057$	$\beta = 0.74883$	$\beta = 0.752023$	$\beta = 0.75632$	$m/\sqrt{\sigma}$	m/m_{0^+}
0^+	3.23(1)	3.18(2)	3.17(1)	3.12(5)	3.08(3)	1
$(0^+)'$	5.85(12)	5.80(6)	5.78(6)	5.79(13)	5.80(4)	1.88(2)
$(0^+)''$	7.8(2)	7.8(2)	8.3(3)	8.4(3)	7.97(11)	2.59(4)
(0^-)	10.0(7)		9.9(8)		10.0(5)	3.25(16)
$(0^-)'$			13.8(6)		13.8(6)	4.48(20)
2^+	7.8(1)	7.9(2)	7.8(3)	8.2(2)	7.88(8)	2.56(4)
2^-	8.0(1)	7.8(2)	8.1(3)	8.6(2)	8.07(8)	2.65(4)
$(2^+)'$	9.3(3)		9.9(5)	10.4(3)	9.86(20)	3.23(7)
$(2^-)'$		10.0(4)	9.9(9)	10.5(5)	10.16(30)	3.33(10)
$1/3$		12.5(6)	12.4(1.6)	12.1(1.1)	12.4(5)	4.07(16)
$(1/3)'$		13.1(6)	12.4(1.6)	13.2(1.3)	13.0(5)	4.26(16)

As already discussed above, our data clearly confirm the degeneration between states of different parity, for $J > 0$.

If we assume this degeneration as an input information we can obtain more precise estimates for the spectrum, fitting together all the 2^+ and 2^- states and the first pair of $1/3$ states. The resulting spectrum is reported in tab.9 .

Besides these states we also obtained estimates for the third excitation in the 2^+ , 2^- , $1/3$ and 0^- channels (see tab.4). However these estimates are affected by a large uncertainty and we did not try to extrapolate a continuum limit value for the corresponding masses.

5.2 The Isgur-Paton model

More than ten years ago Isgur and Paton suggested to describe the glueball spectrum of a generic gauge theory within the framework of a flux tube model. Up to our knowledge this is the only model which also incorporates the effects of the quantum fluctuations of the flux tube in a consistent way (see below). We shall describe the IP model, directly in the (2+1) dimensional case in which we are interested. For a more detailed discussion and for the extension to (3+1) dimensions we refer to the original paper [4] and to [9]. An appealing feature of the IP models is its simplicity.

The starting point is the assumption that the glueballs are “rings of glue”, namely that they are described by thin, oscillating, flux tubes which close upon themselves. This is the natural extension to the glueball case of the flux tube model which describes the mesons as flux tubes which end on quarks. The second, important, assumption of the model is the so called “adiabatic approximation” (which allows to explicitly quantise it). To understand this approximation, let us think for simplicity of a circular flux loop of radius R . It can have two type of fluctuations: phonon-like fluctuations at a fixed radius, and collective radial excitations. In the adiabatic approximation these two types of excitations are treated in a completely different way. The phonons are quantised as free harmonic oscillators, neglecting the radial excitations. Taking into account their contribution we can construct the total energy E_{tot} of the flux loop. Then we quantise the radial excitations using the energy provided by the phonons as a fixed background potential. Thus the problem of finding the mass eigenstates is reduced to the solution of a suitable radial Schrödinger equation in the only remaining variable R . To this end let us first explicitly write E_{tot} . The various phonons can only have frequencies which are multiples of $1/R$. Since the circular loop is embedded in the 2+1 dimensional space, a phonon of frequency m/R will imply an angular momentum for the glueball of $J = \pm m$ (the sign depending on the clockwise or counter-clockwise nature of the phonon). Hence the total angular momentum due to the phonons is

$$J = \sum_m m(n_m^+ - n_m^-) \quad (17)$$

where n_m^+, n_m^- is the number of phonons with angular momentum $+m$ and $-m$ respectively. The corresponding energy is

$$M = \sum_m m(n_m^+ + n_m^-) \quad (18)$$

Some remarks are in order at this point.

- a] The role of the parity operator in this context is to interchange $+$ and $-$ phonons. Thus we see that (for $J > 0$) excitations with the same angular momentum but different parity are degenerate in energy.
- b] As it always happens when looking to the quantum fluctuations of a flux tube, the zero point energy of the oscillators gives a divergent contribution to the total energy. This divergence can be regularized for instance with the ζ function regularization. The resulting, finite, contribution to the total energy is $13\pi/l$ where $l = 2\pi R$ is the loop length. This term is the equivalent in this context of the well known “Lüscher” term which is present in the flux tube models for the interquark potential [2, 3].
- c] In writing the total energy of the flux loop we must also take into account, in analogy to the interquark case, a contribution proportional to the length

of the loop and to the string tension: $2\pi\sigma R$ and the possible existence of a constant term: c_0 .

- d] In the sums of eq.(17,18) we must neglect the $m=1$ phonons, since the oscillations with $m = 1$ are equivalent to infinitesimal rotations and translations. This has the important consequence that it is more difficult to construct a $J = 1$ or $J = 3$ excitation than the $J = 2$ one, which hence has a lower mass. This is indeed confirmed by the simulations and is one of the most appealing results of the IP model. The realization of the various angular momenta, with the smallest possible total energy are listed in tab. 8.

Table 8: *Phonon content of the various glueballs. The states are listed in order of increasing energy. For some states we have listed some possible different realizations.*

J^P	n_2	n_3	n_4	M
0^+	0	0	0	0
2^\pm	1	0	0	2
3^\pm	0	1	0	3
0^+	2	0	0	4
1^\pm	1	1	0	5
0^+	0	2	0	6
2^\pm	1	0	1	6
0^-	2	0	1	8

Taking into account all these features the total energy turns out to be:

$$E_{tot}(R) = 2\pi\sigma R + c_0 + \frac{M - 13/12}{R} \quad (19)$$

However in working out eq.(19) we have considered the flux tube as an “ideal” string without thickness. We know that this is not the case. In fact such finite thickness of the flux tube has been recently observed with high precision exactly in the (2+1) dimensional Ising model that we are studying now [7] and has been found to be (for the range of scales typical of these glueball states) of the order of $\frac{1}{\sqrt{\sigma}}$ (see below for a more detailed discussion). This is actually a general feature of gauge models and a similar behaviour is expected also, for instance, for (3+1) dimensional SU(3) gauge theory. This fact is taken into account in the IP model, following the original suggestion in [4], by introducing a phenomenological parameter f which should soften the $1/R$ divergence as $R \rightarrow 0$. The final form of E_{tot} is thus:

$$E_{tot}(R) = 2\pi\sigma R + c_0 + \frac{M - 13/12}{R} (1 - \exp[-f\sqrt{\sigma}R]) \quad (20)$$

The resulting radial Schrödinger equation can then be solved numerically so as to obtain the glueball spectrum and compare it with the Montecarlo results.

5.3 Comparison with Ising and SU(2) spectra and discussion.

The glueball spectrum that one obtains by solving the Schrödinger equation depends on the two phenomenological parameters c_0 and f , and in principle one could try to tune these parameters so as to fit the results of the Montecarlo data. However there are some features of the model which are largely independent from these parameters and allow to discuss the reliability of the model in a more general way. We have reported in the fourth column of tab.9 the IP spectrum obtained by choosing the “ideal” string model with $f = \infty$ and $c_0 = 0$ ². This could help to follow the forthcoming analysis and the comparison between the IP model and our Montecarlo results.

Let us first distinguish the splitting among different angular momenta from that among different radial excitations at fixed J . The pattern of the states with different angular momenta can be already seen, without solving the Schrödinger equation, looking at the E_{tot} behaviour as a function of J . In fact the E_{tot} pattern is essentially respected by the final mass spectrum. In this respect we can see some peculiar features of the IP model (see tab.8):

- 1] The parity degeneration of the spectrum is present also in the IP model, and is one of its constituent features.
- 2] The lowest excitation (neglecting the radial excitations) above the 0^+ is the 2^\pm , while the 3^\pm doublet (which are the lowest states in the 1/3 family) has a higher mass.
- 3] The 0^- state has a mass which is much larger than that of the 3^\pm doublet.

While the first two features agree very well with the Montecarlo results (and in particular the second point is probably the most appealing feature from a theoretical point of view of the IP model), the third one completely disagrees. Since it is a structural and unavoidable consequence of the IP model, it indicates that some drastic improvement of the model is needed to reach a more realistic description of the glueball pattern³

Let us now turn to the splitting of the radial excitations. By solving the the Schrödinger equation one can see the following features (see tab.9):

- 1] The radial splittings are, in general, smaller than those between different angular momentum families. This agrees with the adiabatic approximation, which

² A suitable tuning of f and c_0 could lead to a better agreement with the Montecarlo results, which however would probably be fictitious and misleading.

³Notice, as a side remark, that the effect of the f parameter is to increase the masses of the 0^+ family and to decrease that of all the other angular momenta, as f is decreased from ∞ to 0. Thus point (3) above is not affected by f .

however should require the radial splitting to be much smaller than the angular momentum one, while in the spectrum the difference is only of a factor of about two.

- 2] The radial splittings show a small monotone dependence on the value of the masses. They become smaller and smaller as the masses increase. Since the overall values of the masses at a fixed J changes as f is changed, also the radial splittings show a corresponding small dependence on f .
- 3] Comparing the splittings predicted by the IP model and those found in the Montecarlo simulation we see that the order of magnitude is essentially the same, the IP ones being in general a bit larger than the Montecarlo ones.

Table 9: Comparison between the Ising, $SU(2)$ and IP spectra. In the last column we report the IP predictions for the glueball radii.

J^P	Ising	$SU(2)$	IP	$R_{max}\sqrt{\sigma}$
0^+	3.08(3)	4.763(31)	2.00	0.50
$(0^+)'$	5.80(4)		5.94	
$(0^+)''$	7.97(11)		8.35	
2^\pm	7.98(8)	7.78(10)	6.36	0.65
$(2^\pm)'$	9.95(20)		8.76	
0^-	10.0(5)	9.90(27)	13.82	1.20
$(0^-)'$	13.8(6)		15.05	
$(1/3)^\pm$	12.7(5)	10.75(50)	8.04	0.75

Looking at tab.9 we see that the major disagreement in the mass values is for the lowest state which is predicted to be too light. This is certainly a consequence of the fact that in this ideal string picture we have introduced no self repulsion term for the flux tube. Thus the lower states, and in particular the 0^+ ground state, are smaller (and consequently lighter) in the IP model than in the actual gauge model. It would be interesting, to test this picture, to have some idea of the “mean radius” of the various glueball. This is indeed possible in the framework of the IP model, since from the numerical solution of the radial Schrödinger equation one can extract not only the eigenstates but also the eigenfunctions of the various glueball states. They give us an idea of the actual sizes of the various glueballs which should coincide with the position R_{max} of the maxima in the corresponding probability distributions . The results for the lowest excitations (with the same choice $c_0 = 0$ and $f = \infty$ as above: “ideal” string), measured in units of $1/\sqrt{\sigma}$ are reported in the last column of tab.9 . These eigenfunctions are plotted (with the radial coordinate measured in units of $1/\sqrt{\sigma}$) in fig.3 for the lowest excitation

in each channel, while in fig.4 we have plotted the first three excitations in the 0^+ channel.

The fact that we have studied in particular the Ising model, allows us to give a somehow more quantitative evidence in favour of the above discussion. In fact a lower bound for the radius at which the free flux tube picture should break down, and some self-interaction of the flux tube must be taken into account, is certainly given by the thickness of the flux tube itself. The value of this thickness has been studied in great detail, in the case of the three dimensional Ising model in [7]. It turns out that the thickness ρ is a function of the length of the tube (in our case $2\pi R$). and that the functional form of the dependence of ρ on R is an universal function which only depends on the type of boundary conditions of the flux tube. In the case in which we are interested the law is [3, 7]:

$$\sigma\rho^2 = \frac{1}{2\pi} \log(2\pi\sqrt{\sigma}R) + b \quad (21)$$

where b is a non-universal constant which depends on the details of the model. In the case of the Ising model this constant has been measured with high precision in [7]. Plugging its value in eq.(21) and choosing $R\sqrt{\sigma} = 0.50$, namely the radius predicted by the IP model for the 0^+ glueball, we find that $\rho\sqrt{\sigma} \sim 0.6$. This gives an independent evidence that exactly for the lowest mass state the flux tube picture must necessarily break down, and that some kind of self-interaction of the flux tube with itself must be taken into account.

The flux tube picture which emerges from the above considerations is strongly supported by the comparison, made in tab.9, with the $SU(2)$ spectra in (2+1) dimensions (data taken from ref.[8, 9]). It is in fact very interesting to see that, again, the major disagreement between the two spectra is in the lowest state, which is the one with the smallest radius, while states with higher mass (and larger size) show a remarkable agreement, not only in the pattern of the various states, but also in their numerical value. As mentioned above, for the lowest state, it is the flux picture itself that breaks down and the gauge group becomes important. On the contrary for the higher states the choice of the gauge group seems to be ininfluent. This observation supports the idea, discussed in the introduction, that these massive spectra share some sort of “super-universality” as a consequence of the fact that their general features are all described by the same flux tube model. This “super-universality” then breaks down exactly when the flux tube picture itself loses its validity. It would be very interesting to test this conjecture with some other glueball spectra in (2+1) dimension.

The overall impression from this analysis is that in general, the idea that the glueball spectrum could be described by some type of flux tube model is strongly supported by our results, and in particular by the fact that the higher states of the spectrum seems to be independent from the gauge group. The IP model, which is the simplest possible realization of such a flux tube, seems able to catch (at least at a qualitative level) some of the relevant features of the glueball spectrum. However

it has also some serious drawbacks which cannot be solved by simply tuning the c_0 and f parameters and certainly require some improvements and new ideas.

6 Conclusions

For the first time we present a detailed study of the glueball-spectrum of the Ising-gauge theory in 2+1 dimensions. The simulations have been performed with a local demon-algorithm in Multi-spin-coding technique. In order to obtain accurate results for the spectrum, and in particular to obtain results for secondary states in a given channel we used the variational technique discussed in refs. [16, 17]. We obtained reliable estimates for 11 masses in total for 5 channels. We compared our Montecarlo results for the 0^+ state with those of biased inhomogeneous differential approximants of a low temperature expansion [19]. The results are consistent, but certainly our MC result is more accurate for β close to criticality. We studied the scaling of the masses with the square root of the string tension and extrapolated their values to the continuum limit. These results were then compared with those obtained in perturbation theory for the (2+1) dimensional ϕ^4 model. We found an excellent agreement, and our error-bars are considerably smaller than those of the estimates obtained with perturbation theory. In order to test the flux-tube picture of the glueball discussed in the introduction we compared our Montecarlo results for the Ising model with masses obtained from the IP model and Montecarlo results for the SU(2) gauge theory [4, 8]. We found a remarkable agreement between the SU(2) and the Ising spectra except for the lowest state 0^+ . We also observed that the IP model is able to describe (at least at a qualitative level) some of the relevant features of the glueball spectrum. These results support the idea that the large distance properties of any (lattice) gauge theory in the confining phase can be described by a very general and simple flux tube model, and that such a picture breaks down on scales comparable with the flux tube thickness, where the self-interaction of the flux tube becomes important. This scale, in the Ising case seems to coincide with that of the 0^+ glueball. The fact of working in (2+1) dimensions allowed us to deal with a simplified theoretical setting and thus to test in a rather rigorous way the IP model, which is the simplest possible realization of a flux tube model. As mentioned above the IP model correctly describes some of the features of the spectrum, however it has also some serious drawbacks which cannot be solved by simply tuning the various phenomenological parameters of the model and certainly require some improvements and new ideas.

Finally it is important to stress that, by means of a suitable duality transformation, all our results are also valid in three dimensional spin Ising model. It would be very interesting to see if the knowledge of the first states of the spectrum could give us some hint toward a better understanding of the three-dimensional Ising model.

Acknowledgements

We thank F.Gliozzi, K.Pinn, P.Provero and S.Vinti for many helpful discussions. M. Hasenbusch expresses his gratitude for support by the Leverhulme Trust under grant 16634-AOZ-R8 and by PPARC.

References

- [1] P. Olesen, *Phys. Lett.* **B 160** (1985) 144.
- [2] M. Lüscher, K. Symanzik, and P. Weisz, *Nucl. Phys.* **B 173** (1980) 365.
- [3] M. Lüscher, *Nucl. Phys.* **B 180** (1981) 317
- [4] N.Isgur and J.Paton, *Phys. Rev.* **D31** (1985) 2910
- [5] For a review of most recent results see for instance:
M. Baker, J.S. Ball, N. Brambilla, G.M. Prospero and F. Zachariasen, preprint hep-ph/9602419 and references therein.
- [6] See for instance: M.Caselle, R.Fiore, F.Gliozzi, P.Provero and S.Vinti, *Int. Journal of Mod. Physics* **6A** (1991) 4885
- [7] M.Caselle, F.Gliozzi, U. Magnea and S.Vinti, *Nucl. Phys.* **B460** (1996) 397.
- [8] M. Teper *Phys. Lett.* **289B** (1992) 115
- [9] T. Moretto and M. Teper, preprint hep-lat/9312035
- [10] M.Caselle and M.Hasenbusch, in preparation
- [11] M. Creutz, *Phys. Rev. Lett.* **50** (1983) 1411,
M. Creutz, G. Bhanot and H. Neuberger, *Nucl. Phys.* **B 235** [FS11] (1984) 417
- [12] K. Rummukainen, *Nucl. Phys.* **B 390** (1993) 621
- [13] R. Ben-Av, D. Kandel, E. Katznelson, P.G. Lauwers and S. Solomon, *J. Stat.Phys.* **58** (1990) 125
- [14] G.Carlino and M.Hasenbusch, in preparation
- [15] M. Henkel, *J.Phys. A* 20 3969 (1987) M.A. Novotny , *Nucl.Phys.B* (proc. suppl.) 20, 122 (1991);
- [16] A.S. Kronfeld *Nucl. Phys.* **B17** (Proceeding Supplement) (1990) 313
- [17] M. Lüscher and U. Wolff, *Nucl. Phys.* **B 339** (1990) 222.

- [18] M. Hamermesh, *Group Theory and its Application to Physical Problems*, Reading Mass.: Addison-Wesley, 1962
- [19] H.Arisue and K.Tabata, Phys. Lett. **B322** (1994) 224; Nucl. Phys. **B435** (1995) 555
- [20] M.E. Fisher and H. Au-Yang, J. Phys. A 12 (1979) 1677
- [21] A.J. Liu and M.E. Fisher, Physica **A 156** (1989) 35
- [22] J.C. Le Guillou and J. Zinn-Justin, Phys. Rev. **B 21** (1980) 3976.
 For a review of most recent results on the critical indices and coupling of the three dimensional Ising model see:
 H.W. Blöte, E. Luijten and J.R. Heringa, J. Phys. **A 28** (1995) 6289, and references therein.
- [23] R. Gupta and P. Tamayo, LAUR-96-93, cond-mat 9601048.
- [24] G. Münster, *Nucl. Phys.* **B 340** (1990) 559
- [25] S.-Y. Zinn and M.E. Fisher, Physica **A 226** (1996) 168
- [26] M.Hasenbusch and K.Pinn, Physica **A192** (1993) 342.
- [27] M.Caselle, R.Fiore, F.Gliozzi, M.Hasenbusch, K.Pinn and S.Vinti, Nucl. Phys. **B432** (1994) 590.

Figure Captions

- Fig.1** Some lattice realizations of the operators discussed in sect. 3.2 . To clarify the role of the various symmetries, for the 2^- and $1/3$ channels we have shown respectively two and four different realizations. For the 0^+ , 0^- and 2^+ only the simplest possible realizations are shown.
- Fig.2** Approximants of ξ at $\beta = 0.75632$ for a large range of $[K/L;M]$. The continuum line and the two dotted lines denote the mean value and the error of our montecarlo estimate : $\xi = 4.64(3)$. The symbols correspond to different values of K . Open circles: $K=4$, squares: $K=5$, black circles: $K=6$, triangles: $K=7$.
- Fig.3** Eigenfunctions obtained with the “ideal string” IP model ($c_0 = 0, f = \infty$) for the lowest excitation in each channel. The radial coordinate is measured in units of $1/\sqrt{\sigma}$. The four curves correspond, in order of increasing radius, to the 0^+ , 2^\pm , 3^\pm and 0^- states.
- Fig.4** Same as fig.3, but for the ground state and the two first radial excitations of the 0^+ channel.

$$0^+ \quad \square \qquad 2^+ \quad \begin{array}{c} \square \\ \square \end{array} - \square$$

$$\begin{array}{c} \begin{array}{c} \square \\ \square \end{array} - \begin{array}{c} \square \\ \square \end{array} + \begin{array}{c} \square \\ \square \end{array} - \begin{array}{c} \square \\ \square \end{array} \end{array}$$

$$0^- \quad - \begin{array}{c} \square \\ \square \end{array} + \begin{array}{c} \square \\ \square \end{array} - \begin{array}{c} \square \\ \square \end{array} + \begin{array}{c} \square \\ \square \end{array}$$

$$\begin{array}{c} \begin{array}{c} \square \\ \square \end{array} - \begin{array}{c} \square \\ \square \end{array} + \begin{array}{c} \square \\ \square \end{array} - \begin{array}{c} \square \\ \square \end{array} \end{array}$$

$$2^- \quad + \begin{array}{c} \square \\ \square \end{array} - \begin{array}{c} \square \\ \square \end{array} + \begin{array}{c} \square \\ \square \end{array} - \begin{array}{c} \square \\ \square \end{array}$$

$$2^- \quad \begin{array}{c} \square \\ \square \end{array} - \begin{array}{c} \square \\ \square \end{array} + \begin{array}{c} \square \\ \square \end{array} - \begin{array}{c} \square \\ \square \end{array}$$

$$\begin{array}{c} \begin{array}{c} \square \\ \square \end{array} - \begin{array}{c} \square \\ \square \end{array} \qquad \begin{array}{c} \square \\ \square \end{array} - \begin{array}{c} \square \\ \square \end{array} \end{array}$$

$$1/3 \quad \begin{array}{c} \begin{array}{c} \square \\ \square \end{array} - \begin{array}{c} \square \\ \square \end{array} \\ \begin{array}{c} \begin{array}{c} \square \\ \square \end{array} - \begin{array}{c} \square \\ \square \end{array} \end{array} \qquad \begin{array}{c} \begin{array}{c} \square \\ \square \end{array} - \begin{array}{c} \square \\ \square \end{array} \\ \begin{array}{c} \begin{array}{c} \square \\ \square \end{array} - \begin{array}{c} \square \\ \square \end{array} \end{array}$$

Fig. 2

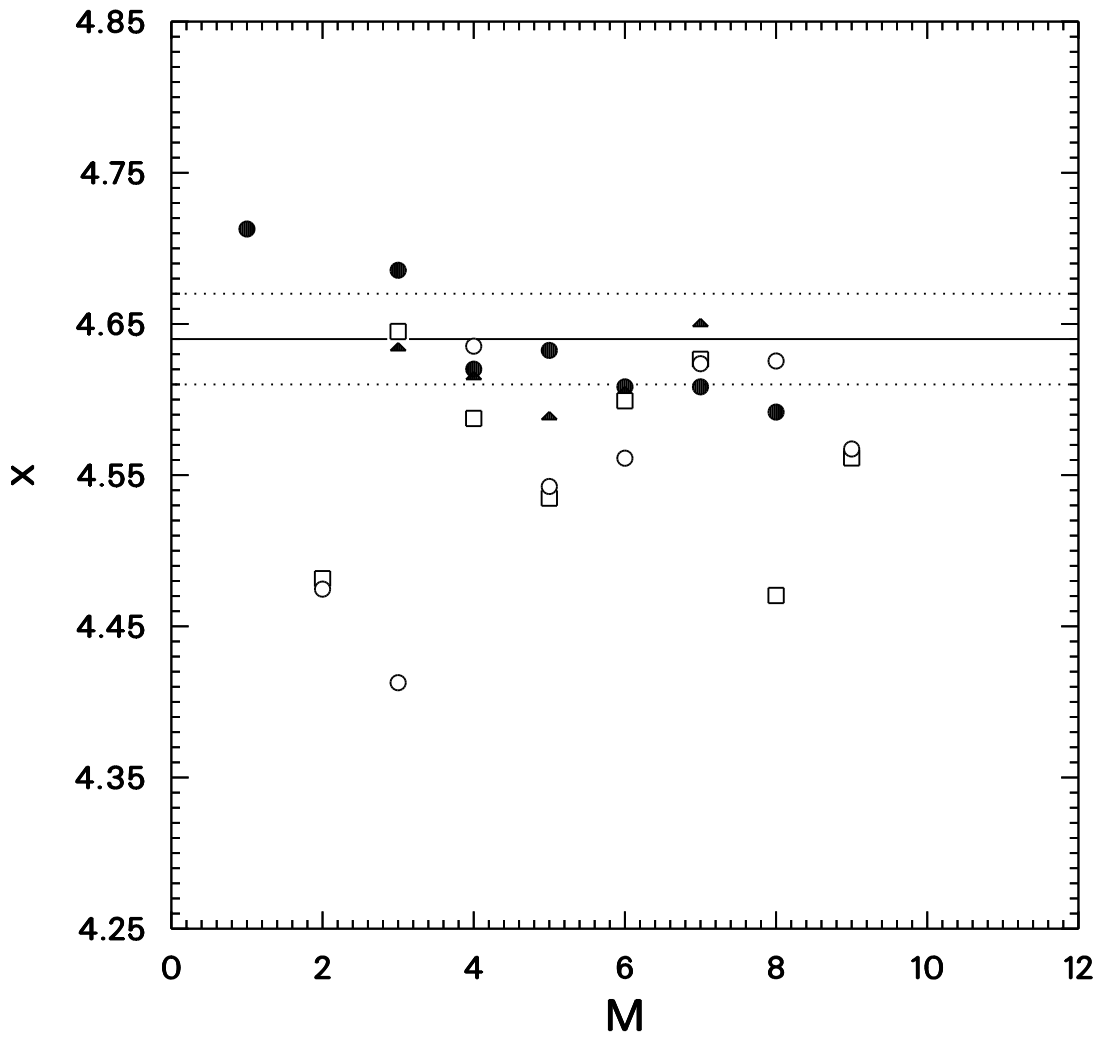


Fig. 3

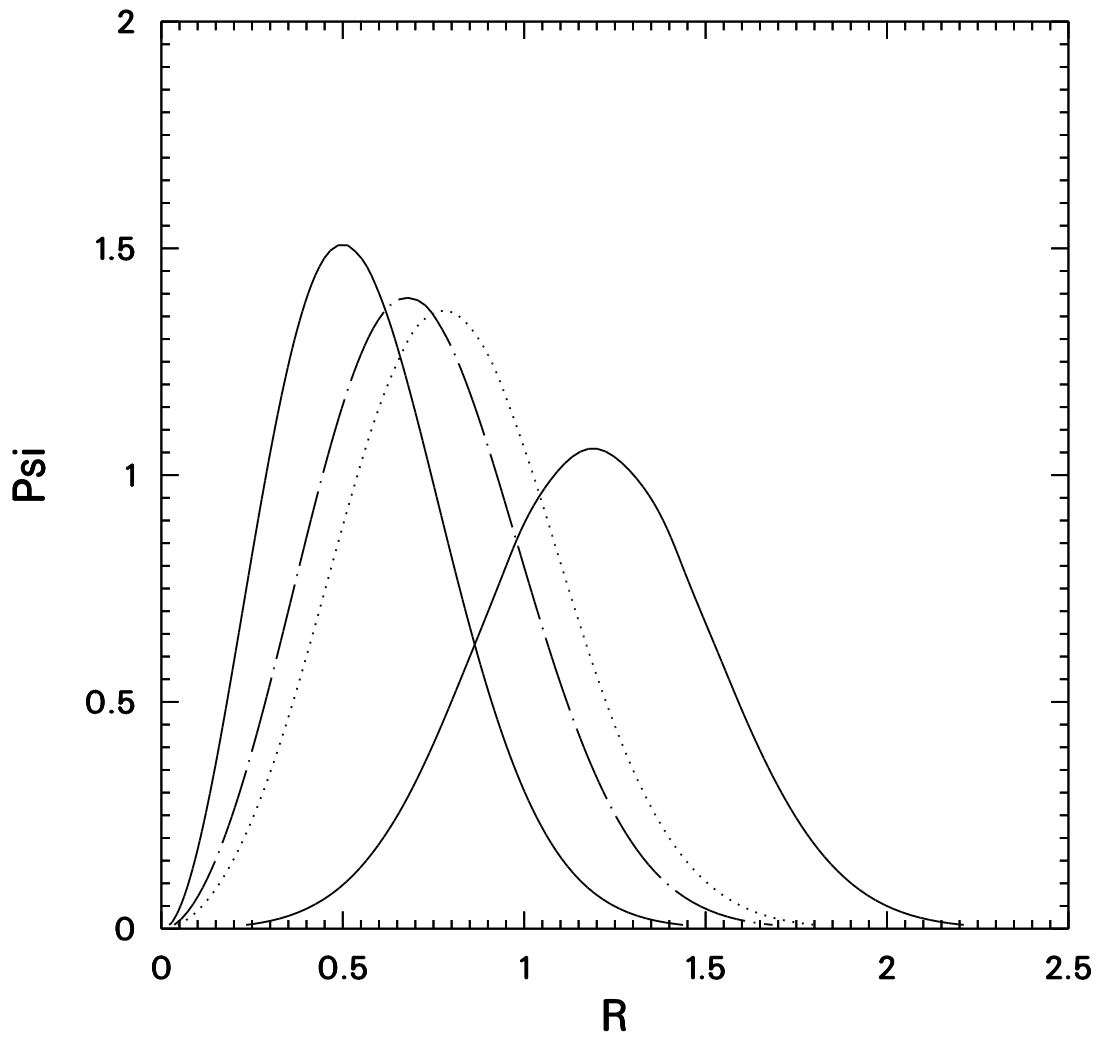


Fig. 4

